Journal of Vacuum Science and Technology A

RESEARCH ARTICLE | MAY 23 2023

Growth mechanisms of interfacial carbon layers at the epitaxial Al_2O_3(0001)/Cu(111) interface as application for epitaxial film lift-off

Hung-Chieh Tsai ; Brecht Marien ; François Chancerel ; Stefan De Gendt ; Steven Brems

Check for updates

J. Vac. Sci. Technol. A 41, 042201 (2023)
https://doi.org/10.1116/6.0002568

View Online
Export Citation

16 April 2024 14:51:44



JVST A
Journal of Vacuum Science & Technology A

ARTICLE

avs.scitation.org/journal/jva

Growth mechanisms of interfacial carbon layers at the epitaxial $Al_2O_3(0001)$/Cu(111) interface as application for epitaxial film lift-off

Cite as: J. Vac. Sci. Technol. A 41, 042201 (2023); doi: 10.1116/6.0002568
Submitted: 8 February 2023 · Accepted: 24 April 2023 ·
Published Online: 23 May 2023

View Online Export Citation CrossMark

Hung-Chieh Tsai,[1,2,a)] Brecht Marien,[1,2] François Chancerel,[2] Stefan De Gendt,[1,2] and Steven Brems[2,b)]

AFFILIATIONS

[1]Department of Chemistry, KU Leuven, Celestijnenlaan 200F, Leuven B-3001, Belgium
[2]Imec, Kapeldreef 75, Leuven B-3001, Belgium

[a)]**Electronic mail:** Hung-Chieh.Tsai@imec.be
[b)]**Electronic mail:** Steven.Brems@imec.be

ABSTRACT

The growth of interfacial carbon (IFC) layers at the epitaxial sapphire/metal interface could unlock the transfer process for large-scale epitaxial thin films, such as graphene. To assess the feasibility of the application of IFC, understanding of the growth mechanisms of IFC layers at the epitaxial metal/sapphire interface is required. In this study, atmospheric pressure chemical vapor deposition is used to directly synthesize wafer-scale multilayer carbon at the interface between the $Al_2O_3(0001)$ substrate and epitaxial Cu(111) layer. Characterization by Raman spectroscopy, AFM, and XRD, indicates the IFC layers exhibit low defect density and sp^2 bonding character. Furthermore, IFC as thick as 100 nm could be synthesized. The effect of the partial pressure of reaction gases is systematically investigated, and a growth mechanism is proposed based supported by experimental observations and simulation results. Finally, a mechanical lift-off of a Cu(111) film with the aid of the IFC layer is demonstrated as a proof-of-concept application.

Published under an exclusive license by the AVS. https://doi.org/10.1116/6.0002568

16 April 2024 14:51:44

I. INTRODUCTION

The unique band structure of graphene keeps drawing attention for electronic applications.[1] Recently, the discovery of the tunable superconductivity of two graphene sheets stacked at a specific "magic-angle" pushes the potential of graphene even further.[2] The requirements for low defect density and precise angle control also highlight the importance of graphene manipulation processes—including the synthesis of high-quality graphene at a large wafer scale and the development of scalable and controllable transfer techniques—to realize its application toward co-integration with matured CMOS, flexible electronics, and sensor technologies. The synthesis of CVD graphene has been intensely explored and oriented epitaxial graphene has been demonstrated on various templates such as a Cu foil[3–6] and epitaxial Cu film.[7–10] Although Cu foils provide a rapid route for graphene processes in a laboratory environment, their surface roughness could limit the transferred graphene quality,[11] and the flexible nature of foils hinders the handling by technology-compatible production tools.

On the other hand, the Cu(111) film epitaxially deposited on c-plane sapphire gains attention as it provides an atomically flat epitaxy template for graphene[7,10] and could be compatible with wafer handling tools in the semiconductor industry. However, the graphene growth process on such substrates is not fully optimized. For instance, a slight temperature fluctuation could lead to interfacial carbon (IFC) layer growth at the Cu/sapphire interface, as shown in this paper.

Furthermore, although various transfer techniques have matured for graphene grown on the Cu foil,[12] the detachment of single-layered graphene (SLG) from the Cu/sapphire substrate is extremely challenging. First, the direct release of SLG from Cu surfaces using techniques, such as electrochemical delamination and PVA peeling, relies on water intercalation between the SLG/Cu interface to reduce the interaction between SLG and Cu.[13–16] However, the low defect density of epitaxial SLG on Cu(111)/sapphire additionally slows down the intercalation process.[13,16] Second, the wet etching process of the catalyst layer (typical

Published under an exclusive license by the AVS

thickness of ~500 nm) between graphene and the substrate wafer is also time-consuming due to the diffusion-limited etching reaction at the etch front of Cu film edges, as the etchant is confined between the submicrometer space between the sapphire substrate and the graphene supporting material.[17] These properties make the transfer techniques developed for Cu foils, which are widely used in laboratory environments, challenging to apply cost-effectively and performance efficient on large-scale Cu/sapphire substrates.

The use of an engineered interfacial layer between sapphire and Cu could help release the Cu-SLG layers from the parent sapphire substrate. Subsequently, the remaining thin Cu layer could be easily etched as the full surface is revealed. Such a release layer could be a low adhesion energy material at the Cu–sapphire interface. This low adhesion layer should weakly interact with the sapphire or/and the Cu film while maintaining the epitaxial relation between all layers and should also withstand the high-temperature graphene growth process. As a possible candidate, carbon (graphene) sheets synthesized at the interface between Cu and sapphire could fulfill these requirements.

Inspired by the studies of direct synthesis of interfacial graphene layers during the CVD process at polycrystal metal/SiO_2 substrates,[18–21] we focus on the IFC growth dynamics on the epitaxial Cu/sapphire system.

Understanding the growth dynamics of an IFC layer could allow further control of epitaxial graphene synthesis. Additionally, it is a direct enabler to a new transfer method that enables a technology-compatible integration route for high-quality graphene and potentially extending the toolbox for 2D material manipulation.

In this study, the direct synthesis of wafer-scale carbon layers at the interface between Al_2O_3(0001) and the epitaxial Cu(111) film by atmospheric pressure chemical vapor deposition (APCVD) is demonstrated. Furthermore, the IFC layer growth mechanism at the Cu(111)/sapphire interface is further investigated by systematically exploring the effect of growth conditions and diffusion modeling. Finally, we performed a proof-of-concept lift-off process to assess the feasibility of using an IFC layer as a release layer.

II. EXPERIMENT

A. Preparation of growth substrate

The details of substrate preparation and characterization of the epitaxial Cu(111)/sapphire are described in our previous work.[7] Polished 2-in. sapphire wafers cut along the c-plane with <1° miscut were used. The as-received wafers were first cleaned in a 3:1 acid mixture of H_2SO_4/ H_3PO_4 at 180 °C for 20 min. The cleaned wafers were then submerged in ultrapure water for 3 min and subsequently, dried by N_2 gas. Immediately after the cleaning process, 500 nm thick Cu (111) films were deposited on the sapphire wafers by a sputtering system (Nimbus XP) with a Cu target (purity 99.995%) at a pressure of 4×10^{-6} mbar with a deposition rate of 3.7 nm/s.

B. IFC layer and single-layer graphene (SLG) growth

The IFC and SLG films were grown in a commercial cold-wall APCVD chamber (Aixtron BM pro 6") with graphite heaters on the top and bottom of the sample. The Cu/ sapphire substrate was placed at the center of a graphite susceptor. The substrate was first annealed in H_2 and Ar gases by ramping the growth temperature to 1050 °C. After reaching the growth temperature, the CH_4 gas was introduced into the chamber. The growth of IFC or SLG was tuned by controlling the partial pressure of each gas while maintaining the total pressure inside the chamber using mass flow controllers. After the growth, the CH_4 gas was closed, and the chamber was cooled down to room temperature at a rate of 10 °C min^{-1} in an Ar/H_2 environment.

The temperature of the sample was monitored by a thermocouple embedded in the susceptor plate and a pyrometer above the sample. During the entire ramping, growth, and cooling period, the chamber pressure was kept at atmospheric pressure.

C. Raman spectroscopy measurements

The Raman spectrum measurements were carried out on the as-grown IFC layer and SLG by using a commercial micro-Raman system (Horiba Labram HR). A 532 nm solid-state laser with a power of 100 mW was used as the excitation source. The laser was focused by a long working distance 50× objective either on the Cu/sapphire interface through double-side polished sapphire wafers to characterize IFC or on the Cu top surface to characterize SLG.

D. IFC surface morphology and thickness characterization

The surface morphology and the thickness of the IFC layers were characterized by the atomic force microscope (AFM) (Bruker Dimension Edge) in ambient using the tapping mode. The IFC at the Cu–sapphire interface was accessible with AFM tip for morphology characterization after removing the Cu film locally by dropping ferric chloride solution at the center of as-grown wafers and rinsing with ultrapure water. The thickness of IFC layers was measured by AFM across a razor blade scratch on the exposed IFC layer on sapphire substrates.

E. X-ray diffraction measurements

The as-deposited Cu/sapphire and as-grown IFC samples were characterized by a commercial x-ray diffraction system (Panalytical X'Pert Pro). The crystalline orientation of the Cu film is analyzed using a Cu Kα source in the Bragg–Brentano configuration. The degree of twinning in Cu(111) layers was determined by measuring Cu{111} phi scan profiles 2-theta angle set to the Cu(111) peak position and tilting the sample at 70.5° (angle between the cubic {111} planes).[7]

F. Determination of growth dynamics

Optical microscopy images were first acquired through the transparent sapphire wafer to determine the density and size of IFC islands. Then, the images were analyzed using ImageJ software. The local density of the IFC layer is determined by retrieving the ratio of the area covered by IFC with respect to the area of the optical microscope image captured at the Cu/sapphire interface through sapphire substrates. The coverage of IFC layers across the entire wafer is determined by recalculating the areal coverage of the IFC relative to the entire wafer. The identification

16 April 2024 14:51:44

Published under an exclusive license by the AVS

of SLG islands grown on the Cu top surface was carried out by heating the as-grown sample on a hot plate at 190 °C in the air for 5 min. The contrast between the oxidized exposed Cu surface and the pristine Cu(111) surface covered with SLG islands can be easily detected in optical microscopy.

G. Transfer peeling of Cu(111) film with IFC

The schematic of the peeling process application of Cu(111) using the IFC is shown in Fig. 4. First, the Cu(111)/IFC/sapphire wafer was cleaved beforehand to enable the initialization of a crack at the interface. Next, thermal release tape (TRT) (Nitto) was laminated on a cleaved IFC-grown Cu(111)/sapphire wafer. The TRT was used as a handle to mechanically peel off the Cu(111) film from the sapphire wafer.

III. RESULTS AND DISCUSSION

A. Synthesis and characterization of the IFC layer

In our previous study, which is consistent with the results of many other groups, the epitaxial single-layer graphene (SLG) growth was demonstrated on epitaxial Cu(111) films deposited on c-plane sapphire.[7,8,10] The as-deposited Cu film was characterized by XRD showing textured Cu(111) with twinning grains. AFM unveiled the as-deposited grain size of 129 nm ± 30 nm.

The standardly used SLG growth conditions are listed in Table I (condition A). After the growth, an epitaxial SLG was obtained on the Cu(111) film surface.[22] The Cu/sapphire interface showed no indications of the presence of carbon deposition.

A slight reduction (or temperature nonuniformity), by 8 °C, in growth temperature (condition A′, Table I) leads to some carbon deposition at the interface. The location of the IFC deposition was found to be closely resembling the mirror image of the location of SLG island growth on the top layer Cu surface [Fig. 2(c)], i.e., the area of "voids" in the IFC deposition corresponded to the area where the SLG islands were grown on the top surface.

By increasing the partial pressure of CH_4 from 0.04 to 3.14 mbar, and H_2 from 17.58 to 393.08 mbar respective to condition A (condition B, Table I), dark carbon deposition was visually observable at the Cu/sapphire interface across the 2-in. wafer [Figs. 1(a) and 1(b)]. Figure 1(a) shows the top surface (Cu/air interface) of the Cu/sapphire sample after IFC growth, while Fig. 1(b) shows the Cu/sapphire interface when the wafer is visualized through the transparent double-side polished sapphire wafer. After IFC growth, a clear dark circular area is visible at the Cu/sapphire interface. An optical microscopy image showed the IFC has a grainlike distribution locally [Fig. 1(c)]. Areas with clean exposed Cu were observed between IFC islands.

Figure 1(e) shows the atomic force microscopy (AFM) image of the IFC, indicating a layered structure with wrinkles on most of the flat terraces. The presence of wrinkles is also in line with the observation of graphene grown directly on sapphire substrates.[23] AFM indicated IFC height variations above 90 nm, which is very large considering the low C solubility in Cu of 8 at. ppm at the graphene growth temperature.[24]

These morphology investigations revealed three levels of nonuniformity of the IFC layer: (1) large-scale (centimeter scale) carbon concentration profile with a reduced carbon content between Cu and sapphire at the edge, (2) local density variation (submillimeter scale) with features corresponding to the shape of top surface SLG islands, and (3) microscale IFC islands distribution.

We attribute the large-scale nonuniformity (1) to a temperature profile (inherent to the deposition tool) over the sapphire/Cu wafer with a lower temperature at the wafer edge related to a temperature gradient in the sample heater. The more localized nonuniformity (2) and (3), however, are considered to be related to growth mechanisms, which will be discussed further in the following paragraphs.

The composition of the IFC layers was characterized by Raman spectroscopy and XRD. The Raman spectra acquired at the interface on IFC deposition through the sapphire substrate showed an intense graphene G peak at 1587.7 cm^{-1} (FWHM of 22.4 cm^{-1}), a 2D band at 2731.6 cm^{-1} (FWHM of 45.1 cm^{-1}), and a D-peak around 1350 cm^{-1}. The Raman spectra revealed that the IFC layer is composed of sp^2-bonded graphenelike carbon. On the other hand, the graphene peaks were completely absent from the spectrum acquired from the Cu top surface [Fig. 1(d)].

The XRD Bragg–Brentano spectrum gathered from the top surface [Fig. 1(f)] shows a sharp Cu(111) peak at 43.3° alongside the Al_2O_3(0006) peak (41.7°), confirming Cu(111) orientation on sapphire. The peak at 26.5° was attributed to graphite (002). The peaks in the azimuthal scan at Cu(111) peak are separated by 60° from each other [Fig. 1(g)], indicating that the epitaxial relation between sapphire and Cu film was conserved during the IFC growth.[7,25]

These features of multilayer graphene in Raman and XRD spectra also agree with the morphology characterized by AFM [Fig. 2(e)].

B. Growth mechanism of IFC layers

To understand the growth mechanism of an IFC layer in order to increase the IFC coverage, the effect of the P_{CH_4}/P_{H_2} gas ratio and growth time on the coverage of carbon at the Cu/sapphire interface were investigated first. For a growth time of 60 min, the local IFC grain density increases from 0% to 97% by increasing the P_{CH_4}/P_{H_2} ratio from 0.004 to 0.015. However, when the gas ratio increases further to 0.025, the IFC density drops to 30% [Fig. 2(a)]. To visualize the evolution of IFC density during growth processes, time series of selected conditions were performed [Fig. 2(b)]. A P_{CH_4}/P_{H_2} ratio of 0.015 (Table I, recipe of condition C), allows for an increase in the local density of the IFC layer gradually from 10% to 97% within 60 min of growth time. On the contrary, a high P_{CH_4}/P_{H_2} ratio of 0.025 (Table I, recipe of condition D) results in an increased IFC density after a growth time of 10–30 min, while the density decreased again significantly after a growth time of 60 min. The reverse growth behavior in the high carbon-to-hydrogen ratio environment hints to multiple competing factors affecting the growth of an IFC layer.

Raman spectra reveal different graphene growth behaviors on the top Cu surface. No graphene was found on the top surface after 60 min growth with a high H_2 flow (low P_{CH_4}/P_{H_2} ratio of

16 April 2024 14:51:44

Published under an exclusive license by the AVS

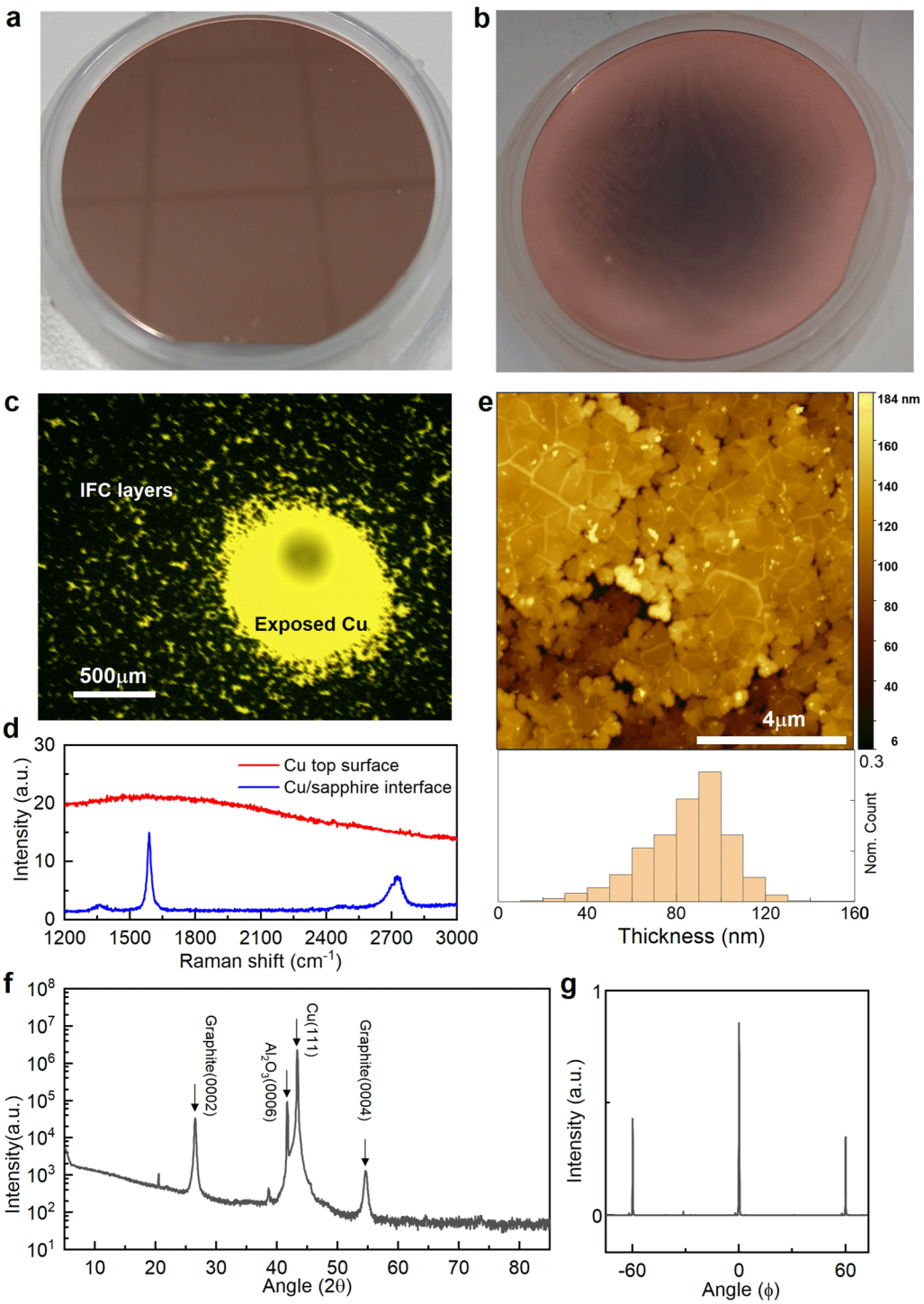

FIG. 1. Characterization of IFC grown in condition B. (a) and (b) The IFC wafer photographs taken (a) from the Cu side and (b) through the sapphire substrate. (c) Representative optical microscope image of the IFC layer. A Cu area with no IFC was included for visualization. (d) Raman spectra from the Cu surface (red) and from the interface through sapphire (blue). (e) AFM micrograph of the IFC layer. Inset: thickness distribution across the entire wafer. (f)–(g) XRD spectra of the (f) $\omega/2\theta$ scan and (g) azimuthal scan of the Cu(111) peak after IFC growth.

16 April 2024 14:51:44

Published under an exclusive license by the AVS

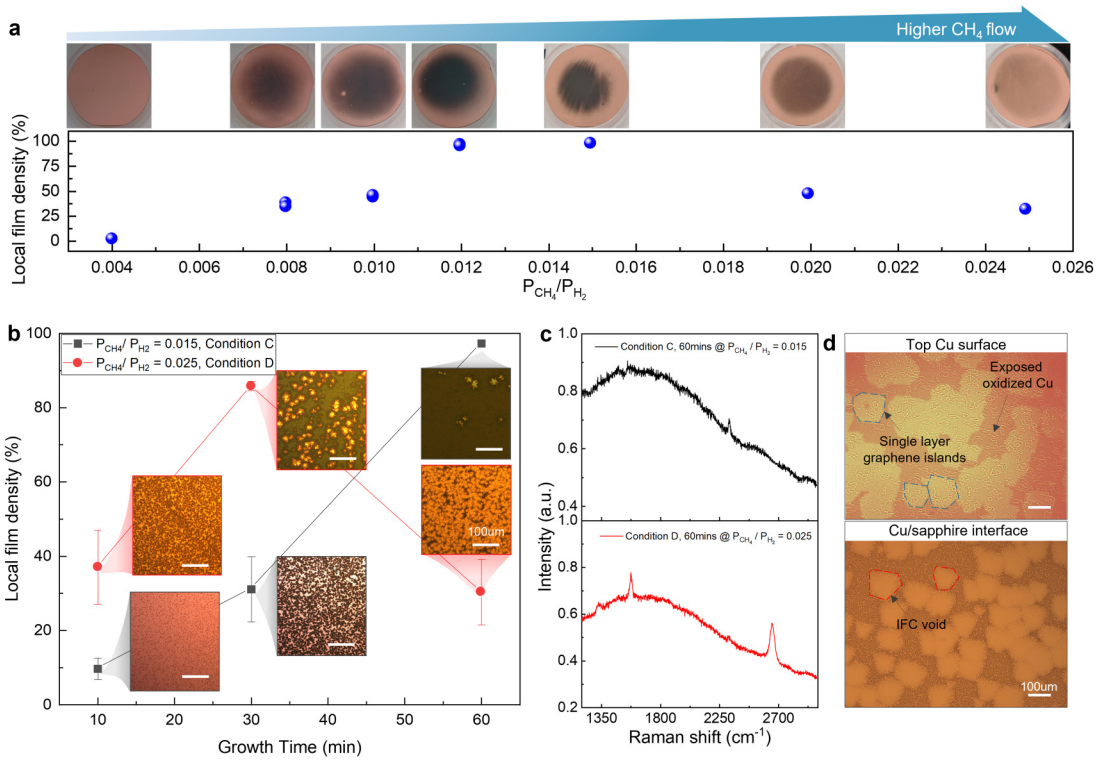

FIG. 2. Growth dynamics of IFC. (a) Dependence of local IFC island density as a function of P_{CH_4}/P_{H_2} for a growth time of 60 min. Representative photographs of the IFC samples are listed above each data point. (b) Time evolution of the local IFC island density for condition C and condition D samples from 10 to 60 min, with corresponding microscope images taken through the sapphire substrate next to the data points (scale bar = 100 um). (c) Raman spectra from the top Cu surface of the samples grown with condition C (top) and condition D (bottom) samples for a growth time of 60 min. (d) Optical images of a sample grown using condition A′ after oxidation in air. The top image shows individual SLG islands from the top Cu surface (enclosed by blue dashed lines). The bottom image shows the Cu/sapphire interface taken through the sapphire substrate, showing clear areas without IFC distribution that followed the shape of SLG islands on the top surface (red dash lines). Scale bar = 100 um.

16 April 2024 14:51:44

0.015—condition C), while the sample grown with a low H_2 flow shows a clear SLG signal on top of Cu(111) [condition D in Fig. 2(c)]. Note that the Raman spectra of the IFC layers measured from the Cu–sapphire interface on these four samples are similar to the representative spectrum shown in Fig. 1(d) (blue curve).

At low CH_4 environment ($P_{CH_4}/P_{H_2} \leq 0.015$), the availability of carbon species that could form IFC could be controlled by the methane pressure. With higher P_{CH_4}, more methane molecules could adsorb to the Cu surface and catalytically decompose into carbon species, resulting in higher surface carbon concentration which drives more carbon species to the Cu/sapphire interface via diffusion.

The lower IFC density at high CH_4 pressure ($0.015 < P_{CH_4}/P_{H_2} \leq 0.025$) can be explained by the observations of the SLG growth on the Cu surface. With a higher P_{CH_4}/P_{H_2} ratio, the formation of IFC at Cu/sapphire interface started to be influenced by the faster formation of SLG on the Cu surface due to a richer CH_4 supply. The SLG formed on the Cu surface could block the

TABLE I. Overview of the growth conditions.

Condition	Pressure (mbar)	Growth time (min)	P_{CH_4} (mbar)	P_{H_2} (mbar)	$\frac{P_{CH_4}}{P_{H_2}}$	Temp. (°C)	Graphene on Cu top surface	IFC at Cu/sapphire interface		
								Presence	Coverage (%)	Film density (%)
A	750	60	0.04	17.58	0.002	1037	SLG[7]	N	—	—
A′	750	60	0.04	17.58	0.002	1029	SLG islands	Y	—	—
B	750	60	3.14	393.08	0.008	1035	N	Y	—	—
C	750	60	5.87	391.64	0.015	1035	N	Y	47	98
D	750	60	9.79	389.61	0.025	1035	SLG and MLG	Y	63	30

Published under an exclusive license by the AVS

dissolution of carbon species into the Cu layer and further diffusion towards the Cu/sapphire interface, reducing the IFC formation rate at the interface. As a result, even with a higher initial IFC growth rate, the carbon concentration at the interface started to reduce once the ambient carbon supply from the ambient was blocked. The carbon at the interface began to diffuse back towards the SLG-covered Cu top surface, forming nonuniformed distributed multilayer graphene at the top surface, which results in the color contrast on the Cu surface and the varying 2D peak intensity in Raman spectra shown in Fig. S1 in the supplementary material.[36]

In contrast, at lower CH_4 environment ($P_{CH_4}/P_{H_2} \leq 0.015$), the relatively higher P_{H_2} leads to a higher SLG etching rate,[25] limits the growth of SLG on the Cu top surface, allowing a continuous entry of carbon toward the Cu/sapphire interface. In this case, the back diffused carbon species would be etched in the hydrogen-rich environment before the rapid cooling freezes the diffusion process. More discussion on the back diffusion of carbon from the interface to the Cu surface can be found in Fig. S1 in the supplementary material.[36]

More discussions regarding the effect of P_{H_2} and P_{CH_4} can be found in Fig. S2 in the supplementary material.[36] Overall, a higher P_{CH_4} increases the coverage area of IFC relative to the entire wafer, while P_{H_2} governs the local density of the IFC layer.

The model of carbon blockage by SLG formation[26] also aligns with the finding in the standard SLG growth condition with a slightly lower temperature [condition A′ and Fig. 2(d)], and in the conditions that carbon back diffusion occurs (Fig. S1 in the supplementary material).[36] Where the void between IFC deposition is correlated to the SLG island on the Cu surface, which indicates that the graphene deposition at the interface was preserved by the growth of the top surface SLG. A similar behavior was also reported in the enclosed Cu foil envelope system, where carbon species can only access the enclosed side of Cu foil by diffusion.[27]

C. Modeling of IFC growth mechanism

To gain a better understanding of the diffusion dynamics of the carbon species from the Cu surface to the interface, we modeled the carbon diffusion dynamics within the Cu film. First, the pathway of diffusion was investigated by estimating the amount of carbon reaching the interface through different diffusion routes, i.e., Cu bulk or internal free surfaces of Cu, such as grain boundaries.

Assuming a steady supply of carbon species from CH_4 gas, a modified Fick's second law can be applied to describe the diffused carbon concentration at a given time t and depth h in the Cu film

$$[C](h,t) = [C_0] \cdot \left(1 - \mathrm{erf}\left(\frac{h}{2\sqrt{Dt}}\right)\right), \quad (1)$$

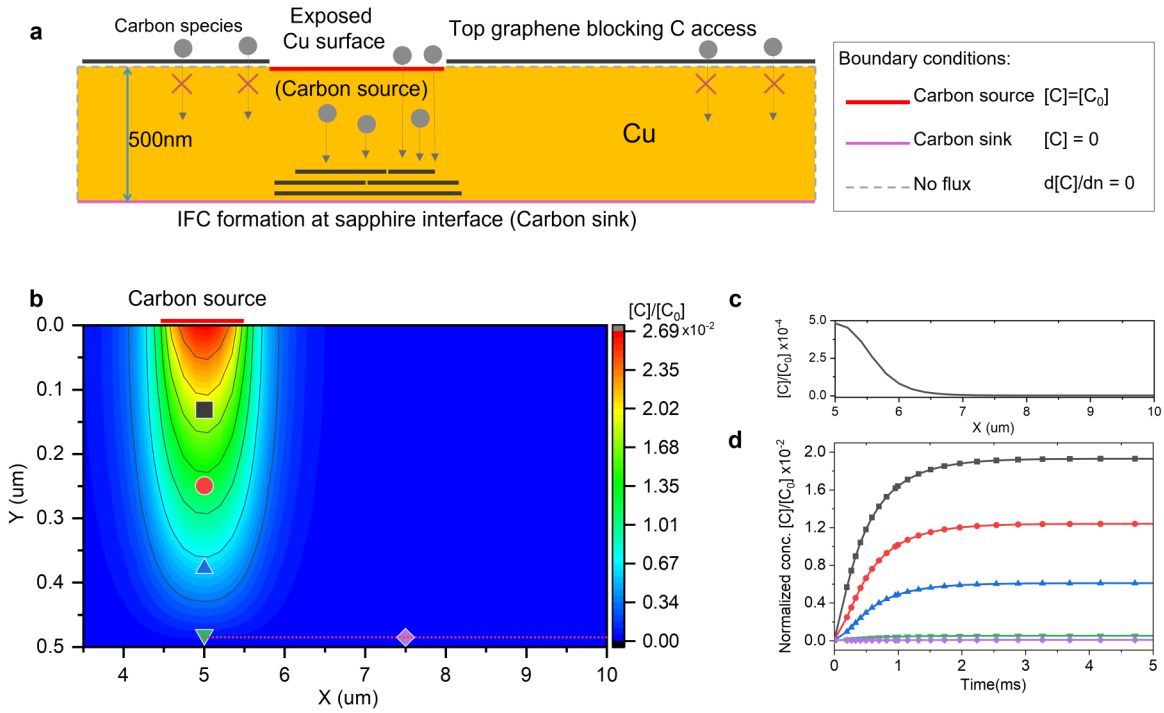

FIG. 3. Carbon diffusion modeling. (a) Schematic of the Cu film model for diffusion analysis. The right panel shows the boundary conditions used in the model. (b) The static-state of the carbon concentration distribution in the Cu film after 10 s. (c) The carbon concentration profile near the Cu/sapphire interface corresponds to the red dashed line in (b). (d) The time evolution of carbon concentration in the Cu film. The sampling positions correspond to the symbols in (b).

16 April 2024 14:51:44

Published under an exclusive license by the AVS

where $[C_0]$ is the concentration of adsorbed carbon species at the Cu surface that could access the diffusion process, D is the diffusion coefficient of carbon in Cu (1.5×10^{-10} m^2 s^{-1} at 1323 K),[28] and the error function $\mathrm{erf}(z) = \frac{2}{\pi}\int_0^z e^{-y^2} dy$. By considering P_{CH_4} as 9.74 mbar, the growth temperature as 1323 K, the adsorbing rate of CH_4 on Cu as 8.74×10^{-3} s^{-1}, the adsorbed carbon concentration on the Cu surface is estimated to be 2.50×10^{-2} ML after 60 mins growth,[29] with 1 ML = 3.85×10^{19} atoms/m^2. Combining the solubility of carbon in bulk Cu around 8 at. ppm[24] gives the carbon concentration that could access the diffusion process $[C_0]$ of 8.8×10^{-7} ML.

According to Eq. (1), at depth h of 500 nm, only a 0.03 ML of carbon layer could be formed at the interface after 1 h at 1323 K if

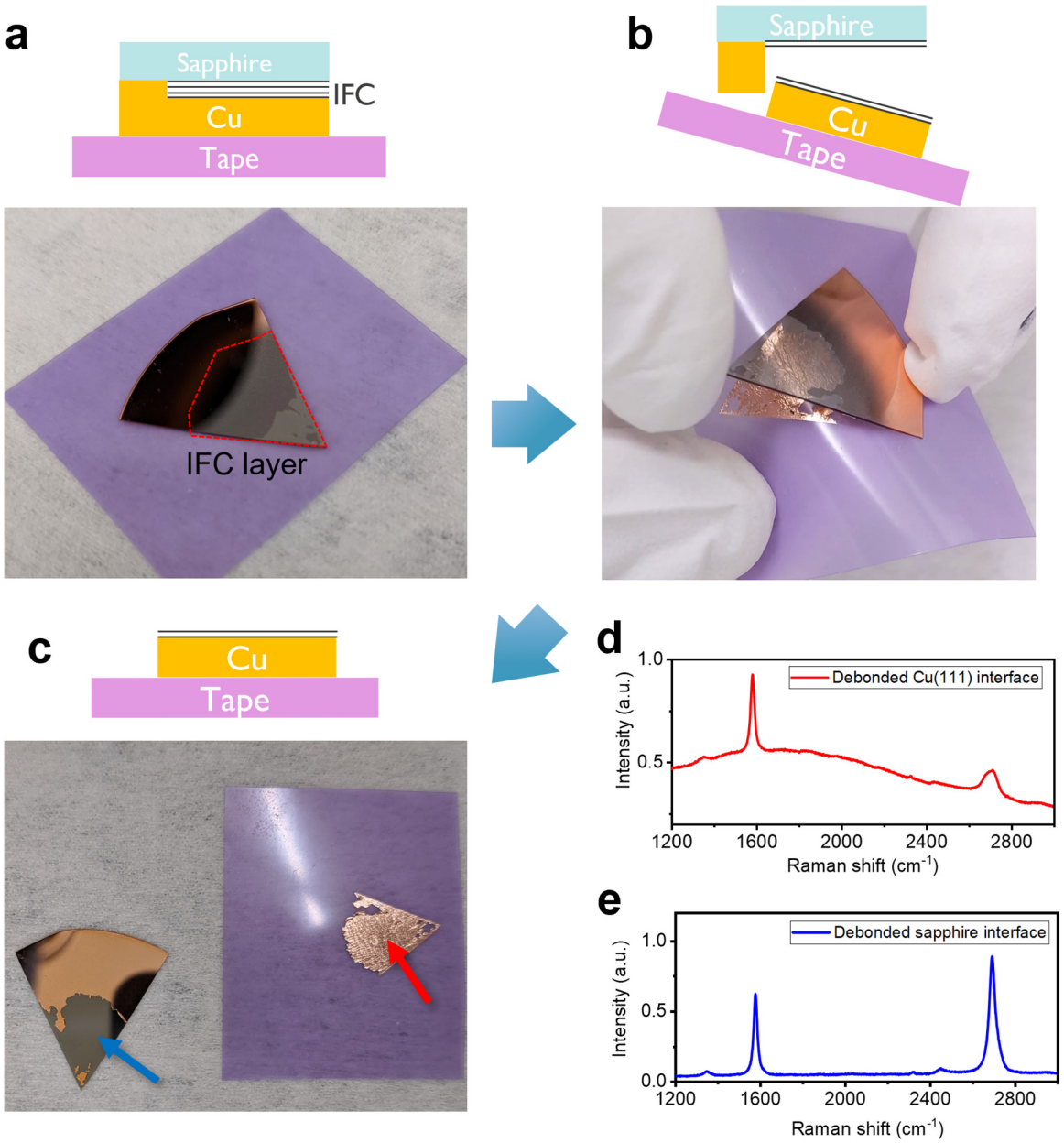

FIG. 4. IFC-assisted Cu(111) film lift-off from a sapphire substrate. (a)–(c) The schematic and the pictures of the peeling process: (a) The IFC coupon attached by a tape, (b) mechanical peeling of the Cu film, and (c) delaminated Cu film on the tape from the IFC-grown area of the sapphire/IFC/Cu coupon. (d) and (e) Raman spectra from (d) the debonded interface of the Cu film and (e) debonded interface on the sapphire substrate as indicated in (c) by the red and blue arrows, respectively.

16 April 2024 14:51:44

Published under an exclusive license by the AVS

the diffusion was fully through bulk Cu (Fig. S3 in the supplementary material).[36] This estimation indicates that to achieve the observed IFC layer, carbon species need another diffusion route. If we consider the adsorbed carbon mainly diffused via free surfaces along Cu defects, the low solubility of carbon in Cu will not limit the diffusion. In this case, the diffusion will be driven by the adsorbed carbon concentration on the Cu surface, i.e., $[C_0] = 2.50 \times 10^{-2}$ ML, which is 5 orders higher than the bulk diffusion. As a result, the carbon reaching the interface could rise to around 90 ML after 1 h of growth. This indicates the carbon deposited at the interface is mainly resulting from the diffusion via Cu defects, for instance, twin boundaries of Cu(111).[18] As shown in our previous study,[7] the as-deposited Cu(111) on sapphire is 60° twinned, with small grain sizes as revealed by XRD and AFM. Before being fully annealed into giant Cu(111) grains during the SLG growth, the grain boundaries could provide pathways for fast carbon diffusion.[7,25] The micrometer scaled twin boundary distribution might also explain the microscale IFC island distribution mentioned above, i.e., the nonuniformity of level (3). The next step is to understand the spatial carbon diffusion dynamics from the Cu surface to the Cu/sapphire interface. Finite element analysis was utilized to simulate carbon diffusion. A localized carbon source was placed on the Cu surface to represent carbon adsorption at the exposed Cu surface between top SLG islands. The Cu/sapphire interface was set as a carbon sink to simulate the consumption of carbon species by forming IFC. The profile of carbon concentration [Figs. 3(b) and 3(c)] shows a sharp reduction in the horizontal direction away from the carbon source. When the boundary condition of the carbon sink at the interface is removed, the distribution of carbon is more uniform across a long distance (Fig. S4 in the supplementary material).[36] This significant difference in carbon distributions between the two simulations indicates the carbon consumption at the interface limits the lateral diffusion of carbon. This result agrees with the observation of the localized distribution of IFC coinciding with areas that are not covered by surface SLG islands [nonuniformity level (2)]. The time evolution of the carbon profile shows the distribution was stabilized within 4 ms [Fig. 3(d)]. This fast diffusion of carbon allowed a constant carbon supply, which depends on P_{CH_4}. Carbon diffuses rapidly to the interface throughout the entire growth period, as long as the Cu surface is not covered by SLG.

To summarize, the simulations reveal that (1) due to the low carbon solubility in Cu, the carbon flux from the top Cu surface to the Cu/sapphire interface is mainly provided by defects in the Cu layer (e.g., twin boundaries), (2) the high carbon diffusivity allows a constant carbon supply, and (3) the consumption of carbon species at the interface confined the lateral carbon diffusion.

D. IFC-assisted epitaxial Cu(111) film lift-off

To illustrate the application of IFC, we demonstrate the delamination of a 500 nm thick epitaxial Cu(111) film from a sapphire(0001) substrate with the assistance of IFC layers at the interface.

As shown in Fig. 4(a), with gentle pressure applied, the Cu (111) film was already detached from one of the corners, indicating the decreasing adhesion between the Cu film and sapphire substrate. By mechanically peeling the TRT, the Cu(111) film within the area where IFC was deposited at the interface can be lifted off from the sapphire substrate. In contrast, the Cu film delamination was not observed in the region at the edge of the wafer without IFC growth. The Raman spectra collected from the delaminated Cu(111) bottom surface and exposed sapphire substrate reveal the existence of graphene layers on both surfaces [Figs. 4(d) and 4(e)]. Indicating the delamination takes place within IFC layers. The Van der Waals interaction between graphene layers in the IFC layer provided an easy route for crack propagation, allowing the separation of the otherwise strongly bond epitaxial Cu(111)-sapphire(0001) interface.

We want to note that the delamination is not yet fully reproducible in a controlled fashion. However, the obtained debonding result demonstrates the feasibility and hints at the need for the development of a more reliable release layer, for instance, improved uniformity of IFC layers. One possible route is to utilize the ion implantation technique. Recently, efforts were made on direct graphene synthesis at the interface of a metal catalyst and a dielectric substrate such as SiO_2.[30] One approach is to implant carbon into the metal films deposited on dielectric, followed by thermal annealing[28,31–33] It could provide better control over the number of graphene layers formed at the interface, as the ion implantation is a nonequilibrium process. The ability to implant carbon species near the interface also could allow a more uniform distribution of IFC islands, as the diffusion path between the implanted carbon source and the interface is shorter.

The fact that our demonstrated delamination happened between the IFC layers also indicates a possible route to fabricate a SLG layer on the sapphire substrate by spalling multilayer graphene grown at the metal–sapphire interface. As shown by Shim *et al.*,[34] the layer-resolved splitting of uniform multilayer graphene grown at the interface is demonstrated by configuring the materials with different interfacial energies on both sides of the interface. This could be a potential way to eliminate the transfer step for graphene on a dielectric substrate once the uniform high-quality IFC layers could be achieved.

IV. CONCLUSIONS

In this study, multilayer graphene was grown at the Cu(111)/sapphire interface directly by APCVD. The role of H_2 and CH_4 partial pressure on the growth dynamics was investigated. Specifically, P_{CH_4} determines the concentration gradient from the Cu top surface to the interface, promotes IFC coverage, while P_{H_2} affects the SLG growth on the Cu top surface. The top surface growth of SLG will block further access to carbon species, leading to a lower IFC density. According to simulation results, the growth mechanism was proposed to be carbon diffusion vertically through the Cu defects, accumulating at the epitaxial interface between Cu and sapphire. In the meantime, the consumption of carbon species by forming IFC limits the lateral diffusion of carbon, resulting in a localized IFC distribution.

The findings indicate the complexity of uniformly controlling IFC growth. While understanding the growth mechanism may be beneficial for other applications, such as controlling the quality of top-surface SLG growth, more straightforward techniques, such as ion implantation of carbon species near the interface, may be more effective for achieving large-scale uniform IFC formation.

16 April 2024 14:51:44

Published under an exclusive license by the AVS

The lift-off of the epitaxial Cu(111) film assisted by the IFC layer was also demonstrated. The result shows that a release layer (e.g., low adhesion layer) between the sapphire wafer and the Cu catalyst layers can be a new route in epitaxial Cu film transfer applications such as high-quality metal contact printing[35] and CMOS-compatible high-quality graphene transfer.

ACKNOWLEDGMENT

This project has received funding from the European Union's Horizon 2020 research and innovation programme under Grant Agreement No. 881603.

AUTHOR DECLARATIONS

Conflict of Interest

The authors have no conflicts to disclose.

Author Contributions

Hung-Chieh Tsai: Conceptualization (equal); Data curation (equal); Formal analysis (equal); Investigation (equal); Writing – original draft (equal); Writing – review & editing (equal). **Brecht Marien:** Data curation (equal); Investigation (equal). **François Chancerel:** Investigation (equal); Writing – review & editing (equal). **Stefan De Gendt:** Conceptualization (equal); Investigation (equal); Project administration (equal); Supervision (equal); Writing – review & editing (equal). **Steven Brems:** Conceptualization (equal); Investigation (equal); Project administration (equal); Supervision (equal); Writing – review & editing (equal).

DATA AVAILABILITY

The data that support the findings of this study are available from the corresponding author upon reasonable request.

REFERENCES

[1]D. Akinwande, C. Huyghebaert, C. H. Wang, M. I. Serna, S. Goossens, L. J. Li, H. S. P. Wong, and F. H. L. Koppens, Nature **573**, 507 (2019).
[2]Y. Cao, V. Fatemi, S. Fang, K. Watanabe, T. Taniguchi, E. Kaxiras, and P. Jarillo-Herrero, Nature **556**, 43 (2018).
[3]X. Xu *et al.*, Sci. Bull. **62**, 1074 (2017).
[4]M. Huang *et al.*, ACS Nano **12**, 6117 (2018).
[5]S. Jin and R. S. Ruoff, APL Mater. **7**, 100905 (2019).
[6]M. Huang *et al.*, Nat. Nanotechnol. **15**, 289 (2020).
[7]K. Verguts, B. Vermeulen, N. Vrancken, K. Schouteden, C. Van Haesendonck, C. Huyghebaert, M. Heyns, S. De Gendt, and S. Brems, J. Phys. Chem. C **120**, 297 (2016).
[8]B. Deng *et al.*, ACS Nano **11**, 12337 (2017).
[9]X. Zhang *et al.*, Small **15**, 1805395 (2019).
[10]D. L. Miller, M. W. Keller, J. M. Shaw, A. N. Chiaramonti, and R. R. Keller, J. Appl. Phys. **112**, 064317 (2012).
[11]B. Huet, J. P. Raskin, D. W. Snyder, and J. M. Redwing, Carbon **163**, 95 (2020).
[12]S. Ullah, X. Yang, H. Q. Ta, M. Hasan, A. Bachmatiuk, K. Tokarska, B. Trzebicka, L. Fu, and M. H. Rummeli, Nano Res. **14**, 3756 (2021).
[13]P. Braeuninger-Weimer, O. J. Burton, P. Zeller, M. Amati, L. Gregoratti, R. S. Weatherup, and S. Hofmann, Chem. Mater. **32**, 7766 (2020).
[14]K. Verguts *et al.*, ACS Appl. Mater. Interfaces **9**, 37484 (2017).
[15]A. Shivayogimath *et al.*, Chem. Mater. **31**, 2328 (2019).
[16]D. Luo *et al.*, Adv. Mater. **33**, 2102697 (2021).
[17]A. T. J. van Niftrik, J. J. Schermer, G. J. Bauhuis, P. Mulder, P. K. Larsen, and J. J. Kelly, J. Electrochem. Soc. **154**, D629 (2007).
[18]C. Y. Su *et al.*, Nano Lett. **11**, 3612 (2011).
[19]T. Kaplas, D. Sharma, and Y. Svirko, Carbon **50**, 1503 (2012).
[20]D. Q. McNerny *et al.*, Sci. Rep. **4**, 5049 (2015).
[21]P. Nguyen, S. K. Behura, M. R. Seacrist, and V. Berry, ACS Appl. Mater. Interfaces **10**, 26517 (2018).
[22]K. Verguts, S. De Gendt, and S. Brems, *Synthesis and Transfer of High-Quality Single-Layer Graphene* (KU Leuven, Faculty of Science, Leuven, 2019), p. 99.
[23]N. Mishra *et al.*, Small **15**, 1904906 (2019).
[24]G. A. López and E. J. Mittemeijer, Scr. Mater. **51**, 1 (2004).
[25]D. L. Miller, M. W. Keller, J. M. Shaw, K. P. Rice, R. R. Keller, and K. M. Diederichsen, AIP Adv. **3**, 082105 (2013).
[26]Y. Zhang, Z. Li, P. Kim, L. Zhang, and C. Zhou, ACS Nano **6**, 126 (2012).
[27]Z. Zhao *et al.*, Small **11**, 1418 (2015).
[28]J. J. Kim, H. Y. Kim, J. H. Jeon, S. An, J. Hong, and J. J. Kim, Appl. Surf. Sci. **451**, 162 (2018).
[29]P. Li, Z. Li, and J. Yang, J. Phys. Chem. C **121**, 25949 (2017).
[30]H. Wang and G. Yu, Adv. Mater. **28**, 4956 (2016).
[31]R. Zhang *et al.*, Appl. Phys. Lett. **102**, 193102 (2013).
[32]D. Chen *et al.*, J. Mater. Sci. **53**, 2631 (2018).
[33]G. Wang *et al.*, Appl. Phys. Lett. **115**, 132104 (2019).
[34]J. Shim *et al.*, Science **362**, 665 (2018).
[35]G. Liu *et al.*, Nat. Electron. **5**, 275 (2022).
[36]See supplementary material online for additional IFC characterization, growth mechanism analysis, and simulation results.

16 April 2024 14:51:44

Published under an exclusive license by the AVS